



Kinetics, thermodynamics, and equilibrium evaluation of adsorptive removal of methylene blue onto natural illitic clay mineral

Duygu Ozdes^a, Celal Duran^{b,*}, Hasan Basri Senturk^b, Hilal Avan^b, Burcin Bicer^b

^aGumushane Vocational School, Gumushane University, 29100 Gumushane, Turkey

^bDepartment of Chemistry, Faculty of Sciences, Karadeniz Technical University, 61080 Trabzon, Türkiye
Tel: +90 462 3774241; Fax: +90 462 3253196; email: cduran@ktu.edu.tr

Received 30 January 2013; Accepted 4 March 2013

ABSTRACT

The natural illitic clay mineral (NICM) has been used as a low cost and highly effective adsorbent in the removal of a toxic cationic dye, methylene blue (MB), from aqueous solution by a batch adsorption technique. The effects of experimental parameters such as initial pH of the aqueous solution, contact time, initial MB concentration, adsorbent concentration, ionic strength, and temperature were studied in detail upon the adsorption process. The process was found to be independent of initial solution pH and the adequate equilibrium time for the adsorption of MB onto NICM was only 60 min. The experimental data were analyzed by the Langmuir, Freundlich, Temkin and Dubinin–Radushkevich isotherm models and showed a good fit with both the Langmuir and Freundlich isotherm models. The monolayer adsorption capacity of NICM was found to be 24.87 mg g⁻¹ by using Langmuir isotherm model. The kinetics of the adsorption were tested using pseudo-first-order, pseudo-second-order, and intraparticle diffusion models. The results showed that the adsorption of MB onto NICM proceeds according to the pseudo-second-order model. Thermodynamic parameters indicated that the present adsorption process was feasible, spontaneous, and endothermic in nature.

Keywords: Illitic clay mineral; Isotherms; Methylene blue; Removal; Thermodynamics

1. Introduction

The discharge of dyes and/or their breakdown products from many industries including textile, paper, cosmetics, pharmaceutical, leather, and plastics may cause significant problems to both environment and living organisms. Methylene blue (MB), a type of cationic dye, is widely employed in dyeing cotton, wool, and silk and it has some harmful effects to living organisms such that the excess intake of MB can

cause increased heart rate, eye burns in humans and animals, shock, Heinz body formation, cyanosis, jaundice, quadriplegia, methemoglobinemia, convulsions, and tissue necrosis in humans, and also if ingested, it damages to the gastrointestinal tract, nausea, vomiting, and diarrhea [1–4]. As most of the dyes, MB has a complex aromatic molecular structure which makes it stable to light, heat, and oxidizing agents [5]. Hence, it is important to develop an efficient method for the removal of MB and also other dyes from waters and wastewaters.

*Corresponding author.

Various alternative methods including adsorption, coagulation and flocculation, precipitation, chemical oxidation, ion exchange, membrane processes, and reverse osmosis have been used for the treatment of dye-contaminated wastewaters. Adsorption technique has been found to be a superior separation and purification method to other methods in terms of its high efficiency, easy handling, high selectivity, and low cost. On the other hand, the regeneration of the adsorbents is easy and the formation of harmful substances is minimized in the adsorption process [6]. In order to further reduce the cost of the adsorption process, there is a demand for the adsorbents which are economical, easily available, having strong affinity, and high loading capacity [7–9]. Therefore, several researchers have focused on the use of effective adsorbents such as de-oiled soya [10], hen feathers [11], bottom ash [12], coconut-husk [13], eggshell waste [14], palm kernel shell-based activated carbon [15], peat moss [16] almond shell [17], magnetite [18], peach palm waste [19], red mud [20], waste mud [21], beach sand [22], laterite [23], and bentonite [24] for the removal of different types of pollutants from waters and wastewaters. Among these adsorbents the clay minerals have been shown to be the most promising alternatives due to their low cost, large specific surface area, high number of negatively charged bonding sites, chemical and mechanical stability, layered structure and high cation exchange capacity [25].

The aim of the present study was to investigate the possible usage of natural illitic clay mineral (NICM) in the removal of MB from aqueous solutions. The effects of experimental parameters such as initial pH of the solution, contact time, initial MB concentration, adsorbent concentration, ionic strength, and temperature were studied in detail upon the adsorption process. The Langmuir, Freundlich, Dubinin–Radushkevich (D–R), and Temkin isotherm models and various thermodynamics parameters, including Gibbs free energy, enthalpy and entropy changes, were also discussed in this paper in order to clarify the adsorption mechanism of MB onto NICM. Apart from these, the adsorption kinetics were evaluated in terms of pseudo-first-order, pseudo-second-order and intraparticle diffusion models.

2. Experimental

2.1. Materials

The NICM sample was supplied from Dazkırı, Afyon/Turkey. The samples were sieved to obtain a particle size of 200 mesh and dried in an oven at 105°C for 24 h and maintained in a desiccator until used.

The NICM was used directly as adsorbent in the adsorption experiments without any physical or chemical pretreatment.

The cationic dye, MB (Fig. 1) (CI: 52015; chemical formula: $C_{16}H_{18}ClN_3S$; molecular weight: $319.86 \text{ g mol}^{-1}$, maximum wavelength: 662 nm) was purchased from Sigma–Aldrich and was not purified prior to use. The stock dye solution was prepared ($5,000 \text{ mg L}^{-1}$) in deionized water and the required concentration of working dye solution was prepared by appropriate dilutions of the stock solutions.

2.2. Characterization of NICM

The X-ray diffraction (XRD) patterns of the samples were taken on a Rigaku D–Max III automated diffractometer using Ni-filtered $\text{Cu K}\alpha$ radiation while the chemical composition of the NICM was determined by Thermo ARL-9800 model X-ray Fluorescence (XRF) Spectrometer and wet analysis. The Fourier Transform Infrared (FTIR) spectrum of the NICM was obtained by using PerkinElmer 1600 FTIR spectrophotometer. The specific surface area of NICM was determined from the N_2 -gas adsorption isotherm at 77 K using a Quantachrome Corporation, Autosorb-1-C/MS model specific surface area analyzer. The cation exchange capacity (CEC) of NICM was calculated by using the copper bisethylenediamine copper (II) ($[\text{Cu}(\text{en})_2]^{2+}$) complex method [26]. Other characterization parameters were also determined using standard methods [27].

2.3. Adsorption experiments

The adsorption experiments were studied by using a batch process by mixing NICM in the concentration range of $1.0\text{--}30 \text{ g L}^{-1}$ with 10 mL of MB solution over the concentration range of $50\text{--}1,000 \text{ mg L}^{-1}$ in polyethylene centrifuge tubes. The mixtures were agitated at a speed of 400 rpm on a mechanical shaker (Edmund Bühler GmbH) for 60 m to reach the equilibrium. After equilibrium, the NICM was separated from the MB solutions by centrifugation and the remaining concentration of MB in the filtrate was determined by using a double-beam UV–Vis spectrophotometer (Unicam–UV 2) at a wavelength of 668 nm.

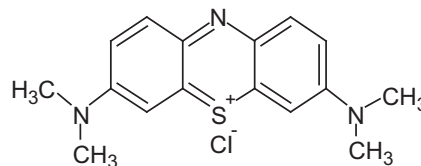


Fig. 1. Chemical structure of MB.

3. Results and discussion

3.1. Characterization of NICM

The significant peaks on the XRD patterns of the samples indicated that the NICM is mainly composed of illite, besides quartz, kaolinite, and smectite (montmorillonite) (Fig. 2). In the FTIR spectrum of the NICM, the absorption bands at $3,624\text{ cm}^{-1}$; hydroxyl group vibrations in Mg–OH–Al, Al–OH–Al, and Fe–OH–Al units in the octahedral layer, $3,440\text{ cm}^{-1}$; O–H stretching vibration of the silanol (Si–OH) groups and HO–H vibration of the water adsorbed silica surface, $1,000\text{ cm}^{-1}$; stretch vibrations of the Si–O groups, $1,430\text{ cm}^{-1}$; stretch vibrations of C=O group, and 530 and 470 cm^{-1} ; asymmetric and symmetric bending modes of O–Si–O groups, were observed (Fig. 3). The information about the pore structure of NICM and other characterization parameters were given in Table 1 [28].

3.2. Effect of initial pH

It is important to discuss the effect of initial solution pH on the adsorption of MB since the concentration of H_3O^+ and OH^- ions affects the adsorption process through the dissociation of the functional groups on the NICM surface. Therefore, the adsorption experiments were carried out with initial MB concentration of 100 mg L^{-1} and NICM concentration of 10 g L^{-1} by varying the pH of the solutions over a

range of 2.0–10.0 (Fig. 4). The uptake of MB by NICM is almost constant in the pH range of 2.0–10.0. Although the constant MB adsorption at all the studied pH range cannot be explained clearly, it is considered that another mode of adsorption, such as ion exchange, may be occurred during the adsorption of MB onto NICM [29]. Also, the adsorption of MB onto NICM might be attributed to weak electrostatic interactions between the dye molecules and the solid surface [30]. Similar results were obtained in the removal of MB from aqueous solution by Neem (*Azadirachta indica*) leaf powder [30]. Hence, further adsorption experiments were carried out at self-pH of MB solution.

3.3. Effect of contact time and evaluation of adsorption kinetics

In order to determine the required contact time to reach the adsorption equilibrium, the experiments were performed by contacting 100 mg L^{-1} of MB solutions with 5.0 g L^{-1} of NICM suspensions in the agitating time range of 1–480 m (Fig. 5(a)). The removal rate was very rapid during the initial stages of the sorption process because a large number of vacant surface sites were available for the adsorption during the initial stage. Thereafter, it continued at a slower rate, and finally reached to equilibrium as a result of saturation of NICM surface sites and also occurrence of the repulsive forces between the MB molecules

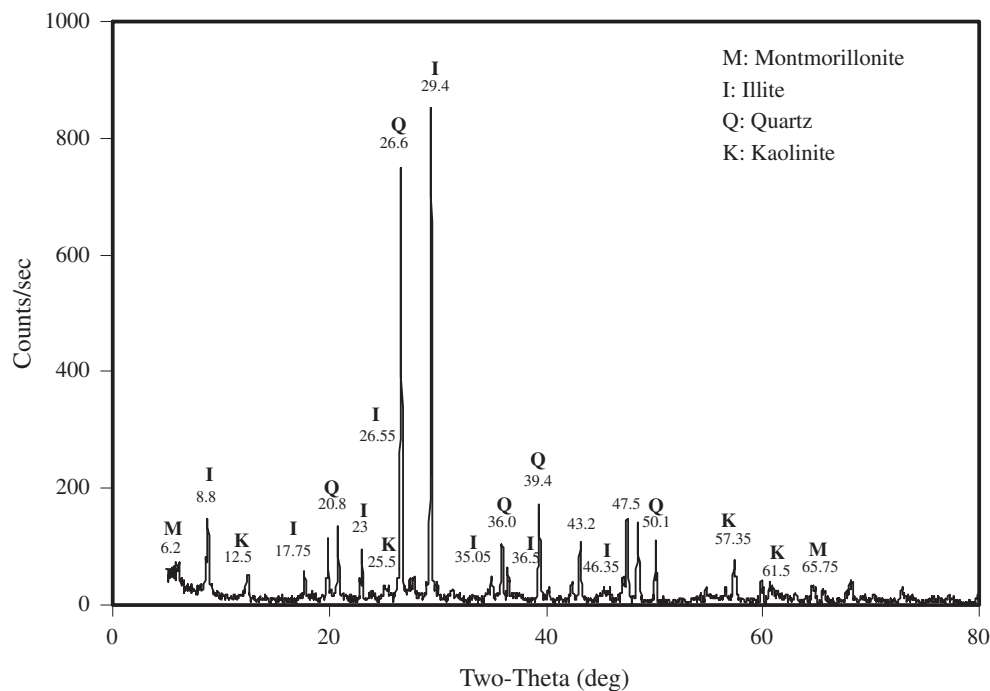


Fig. 2. X-ray diffraction pattern of NICM.

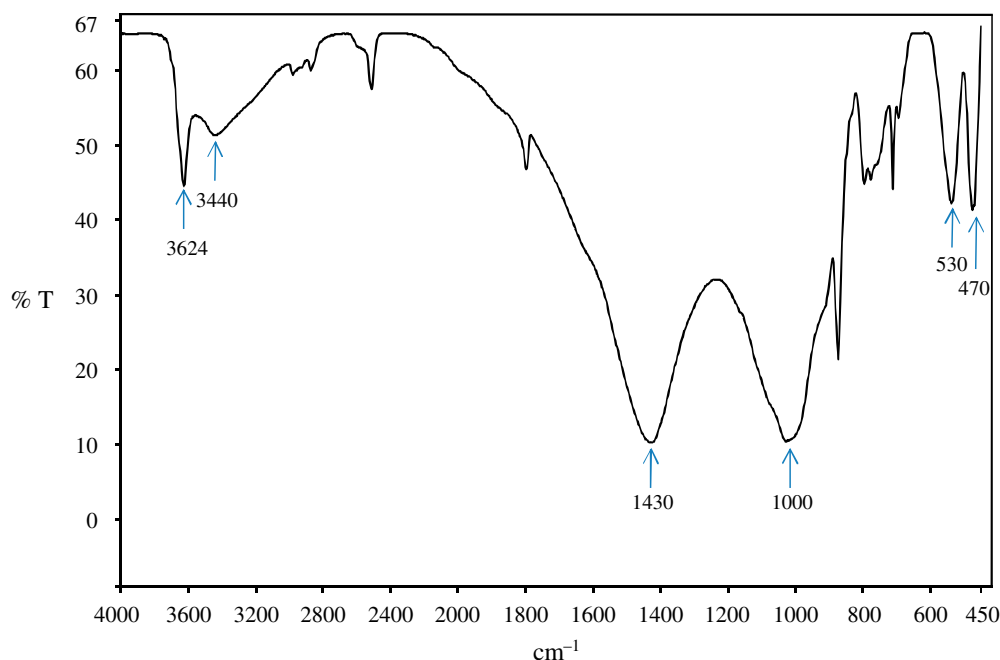


Fig. 3. FTIR spectrum of NICM.

Table 1
Characteristics of NICM

Chemical composition of NICM (%)	
SiO ₂	31.4
Al ₂ O ₃	9.8
Fe ₂ O ₃	4.7
CaO	23.9
MgO	4.1
Na ₂ O	0.7
K ₂ O	1.4
Loss of ignition	23.8
Pore structure of NICM	
BET surface area (m ² g ⁻¹)	3.10
Langmuir surface area (m ² g ⁻¹)	4.64
Micropore area (m ² g ⁻¹)	1.58
External surface area (m ² g ⁻¹)	1.52
Micropore volume (cm ³ g ⁻¹)	0.0008
Average pore diameter (nm)	10.81
Other parameters	
pH	9.6
CEC (meg/100 g)	2.0
Moisture content (%)	1.3

adsorbed onto the NICM surface and the bulk phase [18]. A sufficient contact time was determined as 60 m for further adsorption experiments.

In order to predict the kinetics of dye adsorption, the most common models, pseudo-first-order (Eq. (1))

[31] and pseudo-second-order kinetic models (Eq. (2)) [32], were used to fit the kinetic sorption experiments which are given in linear forms as following:

$$\ln(q_e - q_t) = \ln q_e - k_1 t \quad (1)$$

$$\frac{t}{q_t} = \frac{1}{k_2 q_e^2} + \frac{t}{q_e} \quad (2)$$

By considering the Eq. (1), q_e (mg g⁻¹) and q_t (mg g⁻¹) are the amounts of MB adsorbed at equilibrium and at any time t , respectively, and k_1 (min⁻¹) is the pseudo-first order rate constant. q_e and k_1 can be determined from the intercept and slope of the plot of $\ln(q_e - q_t)$ vs. t , respectively. According to Eq. (2), k_2 (g mg⁻¹ min⁻¹) is the rate constant of the second-order equation. The values of q_e and k_2 can be determined from the slope and intercept of the plot of t/q_t vs. t , respectively (Fig. 5(b)). All of the kinetic parameters constant with the corresponding correlation coefficients were given in Table 2. The correlation coefficient value of the pseudo-second-order kinetic model is higher than 0.999, which is better than those obtained from the pseudo-first-order kinetic model. In addition, $q_{e \text{ cal}}$ determined from the pseudo-first-order kinetic model is not in a good agreement with the experimental value of $q_{e \text{ exp}}$. Furthermore, according to the pseudo-second-order kinetic model, the calculated $q_{e \text{ cal}}$ value is closer to the experimental $q_{e \text{ exp}}$ value. In the view of these results, it can be said

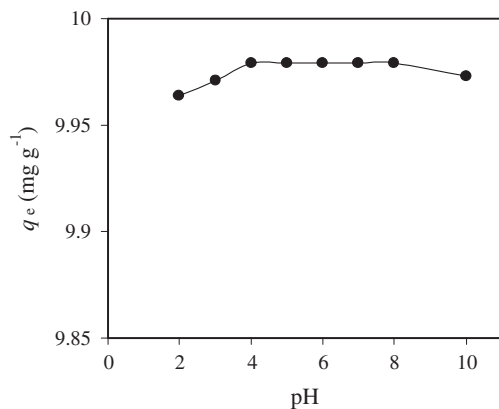


Fig. 4. Effect of initial pH on MB uptake by NICM (Initial MB conc.: 100 mg L^{-1} , NICM conc.: 10 g L^{-1} , contact time: 60 m).

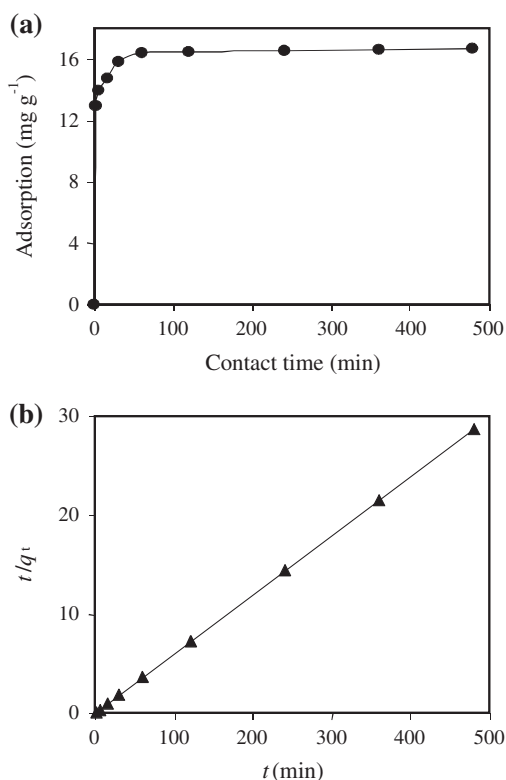


Fig. 5. (a) Effect of contact time on MB uptake, (b) pseudo-second-order kinetic model (Initial MB conc.: 100 mg L^{-1} , NICM conc.: 5.0 g L^{-1}).

that the pseudo-second-order kinetic model provided a good correlation for the adsorption of MB onto NICM in contrast to the pseudo-first-order model and hence, it is predicted that the rate-controlling step in this study is chemical sorption (chemisorption) [33].

The intraparticle diffusion model was also evaluated to investigate the diffusion mechanism of the

adsorption of MB onto NICM. The intraparticle diffusion model equation is expressed as [34];

$$q_t = k_{id} t^{1/2} + c \quad (3)$$

where q_t (mg g^{-1}) is the amount of sorption at time t (min) and k_{id} ($\text{mg g}^{-1} \text{ min}^{-1/2}$) is the rate constant of the intraparticle diffusion model. The magnitude of C gives an idea about the thickness of the boundary layer. The plot of q_t vs. $t^{1/2}$ presents multilinearity (fig not shown) indicating that the adsorption process takes place in two main steps. The first sharper portion is the external surface adsorption (film diffusion) and the second portion is the gradual adsorption stage, where the intraparticle diffusion is rate-controlled (pore or intraparticle diffusion). If the plot of q_t vs. $t^{1/2}$ passes through the origin, the pore diffusion is the only rate-limiting step; if not it is considered that the adsorption process is also controlled by film diffusion in some cases. The intraparticle rate constants for the first phase ($k_{id,1}$) and the second phase ($k_{id,2}$) and C parameters were obtained from the plot of q_t vs. $t^{1/2}$ and the results are given in Table 2. By comparing the rate constants, the lower values of $k_{id,2}$ than $k_{id,1}$ indicate that the rate-limiting step is intraparticle diffusion. The C values, obtained from the intercept of the q_t vs. $t^{1/2}$ plots, indicate that the line did not pass through the origin hence the intraparticle diffusion is not the only rate-limiting mechanism. As a result, it can be said that the adsorption of MB onto NICM is a complex process and both intraparticle diffusion and surface sorption contribute to the rate-limiting step [35,36].

3.4. Effect of initial MB concentration and adsorption isotherms

The initial dye concentration plays an important role in determination of adsorption capacity of an adsorbent. The effects of initial dye concentration on the present adsorption process were evaluated by varying the initial MB concentrations in the range of 50 – $1,000 \text{ mg L}^{-1}$ (Fig. 6). By increasing the initial MB concentration from 50 to $1,000 \text{ mg L}^{-1}$, the MB uptake increased from 10.7 to 24.0 mg g^{-1} since the initial MB concentration acts as a driving force to overcome the mass transfer resistance for the MB transport between the solution and the surface of the NICM. On the other hand, because of the fast saturation of the active adsorption sites on NICM surface at higher MB concentrations, the removal percentage decreased from 92.3 to 14.2% [7].

The adsorption isotherm models are important data in the description of interaction between the

Table 2
Parameters of pseudo-first-order, pseudo-second-order, and intraparticle diffusion models

q_e exp (mg g ⁻¹)	Pseudo-first-order kinetic model		Pseudo-second-order kinetic model		Intraparticle diffusion model						
	k_1 (min ⁻¹)	$q_{e, cal}$ (mg g ⁻¹)	R^2	k_2 (g mg ⁻¹ min ⁻¹)	$q_{e, cal}$ (mg g ⁻¹)	R^2	$k_{id,1}$ (mg g ⁻¹ min ^{-1/2})	R^2	$k_{id,2}$	R^2	C
16.70	-0.0128	2.45	0.7353	0.045	16.72	0.9999	0.507	0.9644	0.018	0.9910	14.19

adsorbate and adsorbent. Several isotherm equations including Langmuir, Freundlich, Temkin and D–R models have been used to describe the equilibrium characteristics of the adsorption of MB onto NICM. The Langmuir model assumes that the adsorption takes place at specific homogeneous sites on the surface of the adsorbent [37] whereas the Freundlich isotherm model is valid for the multilayer adsorption on a heterogeneous adsorbent surface with the sites that have different energies of adsorption [38]. Apart from these, according to the Temkin isotherm model, the heat of the adsorption of all molecules in the layer decreases linearly with the coverage due to adsorbent–adsorbate interactions [39], and lastly the D–R model gives an idea about the type of the adsorption [40].

The Langmuir model in linear form can be given as follows:

$$\frac{C_e}{q_e} = \frac{C_e}{q_{max}} + \frac{1}{bq_{max}} \tag{4}$$

where q_e (mg g⁻¹) is the amount of MB adsorbed per unit mass of NICM, C_e (mg L⁻¹) is the equilibrium MB concentration in aqueous solution, q_{max} (mg g⁻¹) and b (L mg⁻¹) are the Langmuir constants related to the adsorption capacity and free energy or net enthalpy of adsorption, respectively. The q_{max} and b can be evaluated from the slope and intercept of the linear plot of C_e/q_e vs. C_e , respectively.

The favorability of the adsorption process could be predicted by the dimensionless equilibrium parameter R_L , which is defined by the following equation [41]:

$$R_L = \frac{1}{1 + bC_0} \tag{5}$$

where C_0 (mg L⁻¹) is the initial amount of adsorbate and b (L mg⁻¹) is the Langmuir constant described above. The adsorption process can be considered as favorable when R_L value is in the range of 0–1.

The Freundlich model in linear form can be given as follows:

$$\ln q_e = \ln K_f + \frac{1}{n} \ln C_e \tag{6}$$

where K_f is a constant related to the sorption capacity (mg g⁻¹) and $1/n$ is an empirical parameter related to the sorption intensity. The Freundlich parameter, $1/n$, indicates the degree of favorability of the adsorption such that for favorable adsorption process, the value of $1/n$ should be in the range of 0–1. The Freundlich

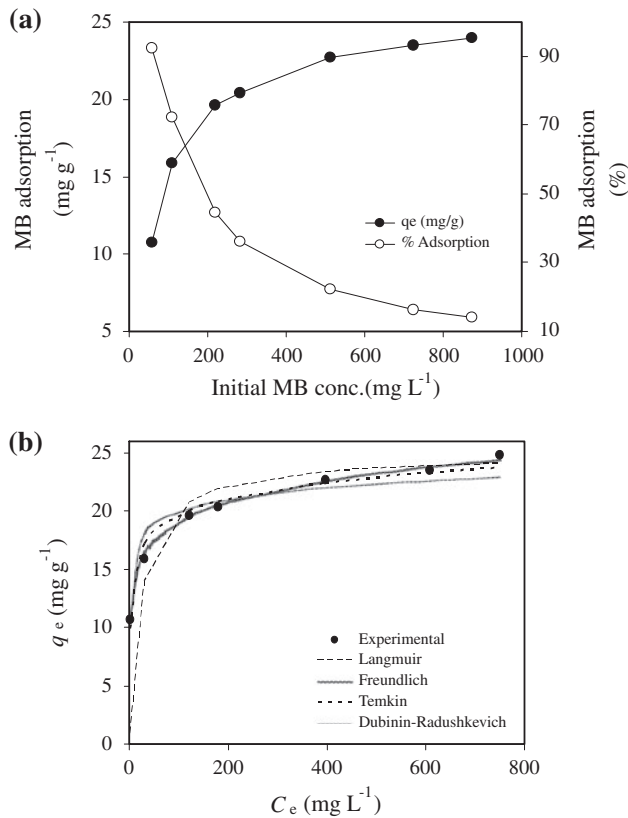


Fig. 6. (a) Effect of MB concentration on its uptake (b) Comparison of equilibrium isotherms between the experimental data and theoretical data for MB uptake (NICM conc.: 5.0 g L⁻¹, contact time: 60 m).

constants, K_f and $1/n$, can be determined from the intercept and slope of the linear plot of $\ln q_e$ vs. $\ln C_e$, respectively.

The Temkin isotherm in linear form is given as

$$q_e = B(\ln A) + B(\ln C_e) \quad (7)$$

$$B = RT/b \quad (8)$$

where B (J mol⁻¹) is the Temkin constant related to the heat of the adsorption, A (L g⁻¹) is the equilibrium binding constant corresponding to the maximum binding energy, R (8.314 J mol⁻¹ K⁻¹) is the universal gas constant, and T (Kelvin) is the absolute solution temperature. The Temkin constants A and B can be determined from the intercept and slope of the linear plot of q_e vs. $\ln C_e$, respectively.

The linear form of D–R isotherm model is expressed as

$$\ln q_e = \ln q_m - \beta \varepsilon^2 \quad (9)$$

where q_e (mol g⁻¹) is the amount of MB adsorbed onto per unit mass of NICM, q_m (mol g⁻¹) is the monolayer adsorption capacity, β (mol² kJ⁻²) is the activity coefficient related to the mean sorption energy, and ε is the Polanyi potential and can be calculated as following equation:

$$\varepsilon = RT \ln(1 + 1/C_e) \quad (10)$$

where C_e (mol L⁻¹) is the equilibrium MB concentration in aqueous solution. The mean adsorption energy, E (kJ mol⁻¹), can be calculated using the following equation:

$$E = 1/(-2\beta)^{1/2} \quad (11)$$

The D–R model constants, q_m and β , can be determined from the intercept and slope of the linear plot of $\ln q_e$ vs. ε^2 , respectively.

The experimental equilibrium data of MB (Fig. 6 (b)) were compared with the theoretical equilibrium data obtained from the Langmuir, Freundlich, Temkin, and D–R isotherm models. The linear graphics of C_e/q_e vs. C_e (for Langmuir isotherm model), $\ln q_e$ vs. $\ln C_e$ (for Freundlich isotherm model), q_e vs. $\ln C_e$ (for Temkin isotherm model), $\ln q_e$ vs. ε^2 (for D–R isotherm model) were plotted in order to calculate the isotherm constants (figs not shown). All of the isotherm constants and correlation coefficients are given in Table 3. The correlation coefficients obtained for both Langmuir and Freundlich isotherm models were higher than those obtained for Temkin and D–R models, which indicated the homogeneous and heterogeneous distribution of the active adsorption sites on the surface of the NICM. The adsorption capacity of NICM was found to be 24.87 mg g⁻¹ by using the Langmuir model equation. The R_L values ranged from 0.32 to 0.02 between 50 and 1,000 mg L⁻¹ of initial MB concentration, and apart from this, the $1/n$ value obtained from Freundlich isotherm model was 0.12. These two results supported the favorability of the adsorption of MB onto NICM. The E value obtained by evaluating D–R isotherm model gives information about the adsorption mechanism such that if the magnitude of E is between 8 and 16 kJ mol⁻¹, the adsorption process takes places chemically while, when $E < 8$ kJ mol⁻¹, the adsorption process proceeds physically [42]. In the present adsorption process, the E value was obtained too high (25.0 kJ mol⁻¹). It is substantially may be the reason of chemical nature of the process.

3.5. Effect of temperature and thermodynamics of adsorption

To investigate the effect of temperature, the adsorption experiments were performed in the temperature ranges of 5–40 °C with NICM concentration of 5.0 g L⁻¹ and initial MB concentration of 100 mg L⁻¹. The experimental results indicated that the amount of adsorption increases slightly with the increase in temperature, suggesting that the adsorption process was endothermic in nature (Fig. 7). At higher temperatures, the viscosity of the concentrated suspensions decreases and hence the diffusion of the adsorbate molecules across the external boundary layer and in the internal pores of the adsorbent particles occurs more easily. In other words, the increase in the mobility of MB molecules may cause an increase in the adsorption amount at higher temperatures [43].

In order to determine whether the adsorption of MB onto NICM will occur spontaneously or not, a set of thermodynamic parameters such as Gibbs free energy (ΔG), enthalpy (ΔH), and entropy (ΔS) changes were calculated. ΔG can be calculated from the following equation [44]:

$$\Delta G = -RT \ln K_d \quad (12)$$

where R is the universal gas constant (8.314 J mol⁻¹K⁻¹), T is the temperature (K), and K_d is the distribution coefficient. The K_d value was calculated using following equation:

$$K_d = q_e / C_e \quad (13)$$

where q_e and C_e are the equilibrium concentration of MB on adsorbent (mg L⁻¹) and in the solution (mg L⁻¹), respectively. The enthalpy change (ΔH), and entropy change (ΔS) of adsorption are estimated from the following equation:

$$\Delta G = \Delta H - T\Delta S \quad (14)$$

This equation can be written as

$$\ln K_d = \frac{\Delta S}{R} - \frac{\Delta H}{RT} \quad (15)$$

ΔH and ΔS values were calculated from the slope and intercept of the van't Hoff plot of $\ln K_d$ vs. $1/T$, respectively. The thermodynamic parameters for the adsorption of MB onto NICM are given in Table 4. The negative values of ΔG at all temperatures indicated the feasibility and spontaneous nature of the adsorption process. In addition, the increase in the magnitude of ΔG with an increase in temperature indicated that a better adsorption is actually obtained at higher temperatures [45]. Generally, it is considered that an electrostatic interaction between the active adsorption sites on the adsorbent surface and the adsorbate molecules (physical adsorption) exists when the ΔG values are in between 0 and -20 kJ mol⁻¹, however, while ΔG values range from -80 to -400 kJ mol⁻¹, the adsorption involves charge sharing or transferring from the adsorbent surface to the adsorbate molecules to form a coordinate bond (chemisorption) [46,47]. By evaluating the ΔG values (between 4.05 and 5.00 kJ mol⁻¹) the adsorption of MB onto NICM seems to be a physical adsorption. The

Table 3
Langmuir, Freundlich, Temkin, and D-R isotherm parameters for the adsorption of MB onto NICM

Langmuir isotherm model	
q_{\max} (mg g ⁻¹)	24.87
b (L mg ⁻¹)	0.042
R^2	0.997
Freundlich isotherm model	
K_f (mg g ⁻¹)	10.73
n	8.06
R^2	0.997
Temkin isotherm model	
A (L g ⁻¹)	138.40
B	2.06
b (J mol ⁻¹)	1202.70
R^2	0.974
D-R isotherm model	
q_m (mg g ⁻¹)	27.44
β (kJ ² mol ⁻²)	0.0008
E (kJ mol ⁻¹)	25.0
R^2	0.933

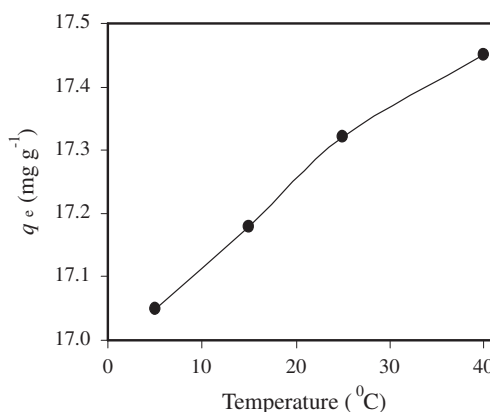


Fig. 7. Effect of temperature on MB uptake (initial MB conc.: 100 mg L⁻¹, NICM conc.: 5.0 g L⁻¹, contact time: 60 min).

positive value of ΔH showed the endothermic nature of adsorption while the positive value of ΔS implied the increased randomness at the solid solution interface during the adsorption of MB onto NICM and also reflected the affinity of the NICM material towards MB. The small positive value of ΔH (3.54 kJ mol^{-1}) also supported physical nature of the adsorption process which involves weak attractive forces [17].

3.6. Effect of adsorbent concentration

The effect of NICM concentration on the uptake of MB from aqueous solution was studied by using initial MB concentration of 100 mg L^{-1} and varying AS concentration from 1.0 to 30.0 g L^{-1} . The equilibrium adsorption amount (mg g^{-1}) and MB removal efficiency (%) against adsorbent concentration (g L^{-1}) were plotted (Fig. 8). As the NICM concentration was increased from 1.0 to 30.0 g L^{-1} , the percentage of the amount of adsorption increased from 81.4 to 99.0% , by virtue of increased in the number of adsorbent particles and thus MB adsorbed easily onto the active adsorption sites. On the other hand for an increase in NICM amount from 1.0 to 30.0 g L^{-1} , the MB uptake decreased from 81.4 to 3.3 mg g^{-1} . This result can be explained by the fact that the increase in the adsorbent amount may lead to aggregate the adsorption sites, resulting in decrease in the total available surface area of NICM [48].

3.7. Effect of ionic strength

The textile-manufacturing wastewaters usually contain various types of ions besides dyestuffs which lead to high ionic strength and may significantly affect the performance of the adsorption process. Hence, the effect of ionic strength upon the uptake of MB was studied by adding different concentrations of (in the range of 0 – 1.0 M) NaNO_3 , Na_2SO_4 , KCl and CaCl_2 solutions individually, in 100 mg L^{-1} of MB solutions,

containing 5.0 g L^{-1} of NICM, and the present adsorption process was applied to these solutions. The presence of salts in the solution may have two opposite effects. One of them is; the presence of ions may screen the electrostatic interaction between the active adsorption sites on the adsorbent and the dye molecules, hence the adsorbed amount should decrease with increase of salt concentration. This result has been shown by evaluating the effect of Na_2SO_4 salt. By increasing the Na_2SO_4 concentration from 0 to 1.0 M , the adsorption efficiency decreased from 16.4 to 16.1 mg g^{-1} .

On the other hand, the ionic strength may cause an increase in the degree of dissociation of the dye molecules by facilitating the protonation. The dissociated dye ions break free for binding electrostatically on the surface of adsorbent and so the adsorption amount increases by the increase in ionic strength [49–51]. These results have been shown by evaluating the effects of NaNO_3 , KCl , and CaCl_2 salts. By increasing the NaNO_3 , KCl , and CaCl_2 salts concentration from 0 to 1.0 M , the adsorption efficiency increased from 16.4 to 16.9 mg g^{-1} , from 16.4 to 18.6 mg g^{-1} , and from 16.4 to 18.7 mg g^{-1} , respectively (Fig. 9).

4. Conclusions

In the present research, the adsorptive removal of MB from aqueous solution was investigated by using a NICM which is one of the most promising adsorbent due to its low cost, easy availability, high specific surface area, and chemical and mechanical stability. One of the essential features of this study was to use the clay mineral without any previous activation treatment which decreases the adsorption costs down. As a result of analyzing the experimen-

Table 4
Thermodynamic parameters of MB adsorption onto NICM at different temperatures

Thermodynamics parameters			
T ($^{\circ}\text{C}$)	ΔG (kJ mol^{-1})	ΔS ($\text{J mol}^{-1}\text{K}^{-1}$) ^a	ΔH (kJ mol^{-1}) ^a
5	-4.05	27.32	3.54
15	-4.33		
25	-4.62		
40	-5.00		

^aMeasured between 278 and 313 K.

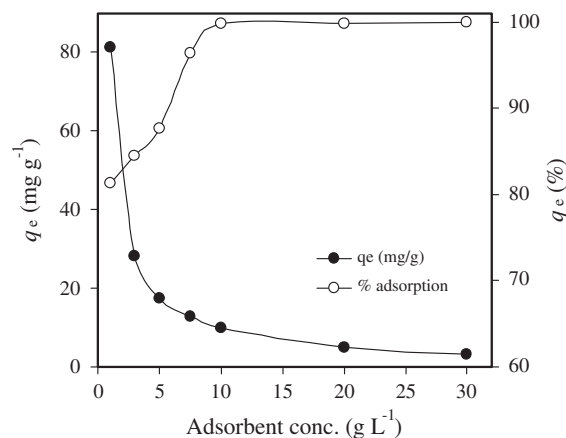


Fig. 8. Effect of NICM concentration on MB uptake (initial MB conc.: 100 mg L^{-1} , contact time: 60 m).

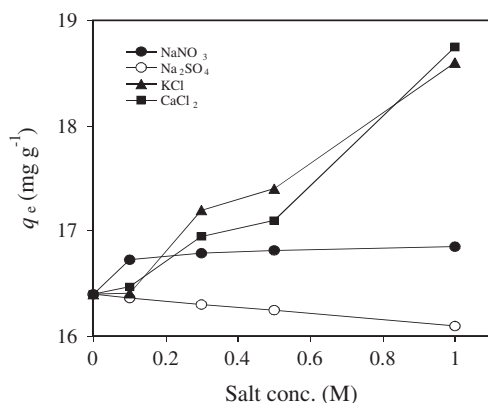


Fig. 9. Effect of ionic strength on MB uptake (initial MB conc.: 100 mg L^{-1} , NICM conc.: 5.0 g L^{-1} , contact time: 60 m).

tal data in terms of isotherm and kinetic models, it is seen that the kinetics of MB adsorption onto NICM followed by pseudo-second-order kinetic model, and the best-fit adsorption isotherms were achieved with the Langmuir and Freundlich isotherm models. The monolayer adsorption capacity of NICM was found to be 24.87 mg g^{-1} from Langmuir model equations. The thermodynamic parameters indicated that the adsorption of MB onto NICM was feasible, spontaneous, and endothermic in nature. In a conclusion, it can be said that the NICM can be used efficiently in the removal of MB from aqueous solutions by using the present adsorption process.

References

- [1] M.R. Sills, W.H. Zinkham, Methylene blue-induced heinz body hemolytic anemia, *Arch. Pediatr. Adolesc. Med.* 148 (1994) 306–310.
- [2] P.K. Gillman, Methylene blue and serotonin toxicity: Definite causal link, *Psychosomatics* 51 (2010) 448–449.
- [3] S.S. Auerbach, D.W. Bristol, J.C. Peckham, G.S. Travlos, C.D. Hébert, R.S. Chhabra, Toxicity and carcinogenicity studies of methylene blue trihydrate in F344N rats and B6C3F1 mice, *Food Chem. Toxicol.* 48 (2010) 169–177.
- [4] A. Majithia, M.P. Stearns, Methylene blue toxicity following infusion to localize parathyroid adenoma, *J. Laryngol. Otol.* 120 (2006) 138–140.
- [5] Md. T. Uddin, Md. Rukanuzzaman, Md. M.R. Khan, Md. A. Islam, Adsorption of methylene blue from aqueous solution by jackfruit (*Artocarpus heterophyllus*) leaf powder: A fixed-bed column study, *J. Environ. Manage.* 90 (2009) 3443–3450.
- [6] A.N. Fernandes, C.A.P. Almeida, N.A. Debacher, M.M.S. Sierra, Isotherm and thermodynamic data of adsorption of methylene blue from aqueous solution onto peat, *J. Mol. Struct.* 982 (2010) 62–65.
- [7] P. Sharma, R. Kaur, C. Baskar, W. Chung, Removal of methylene blue from aqueous waste using rice husk and rice husk ash, *Desalination* 259 (2010) 249–257.
- [8] A. Mittal, V. Gajbe, J. Mittal, Removal and recovery of hazardous triphenylmethane dye, Methyl Violet through adsorption over granulated waste materials, *J. Hazard. Mater.* 150 (2008) 364–375.
- [9] A. Mittal, D. Kaur, A. Malviya, J. Mittal, V.K. Gupta, Adsorption studies on the removal of coloring agent phenol red from wastewater using waste materials as adsorbents, *J. Colloid. Interf. Sci.* 337 (2009) 345–354.
- [10] A. Mittal, D. Jhare, J. Mittal, Adsorption of hazardous dye Eosin Yellow from aqueous solution onto waste material de-oiled soya: Isotherm, kinetics and bulk removal, *J. Mol. Liq.* 179 (2013) 133–140.
- [11] A. Mittal, V. Thakur, V. Gajbe, Evaluation of adsorption characteristics of an anionic azo dye brilliant yellow onto hen feathers in aqueous solutions, *Environ. Sci. Pollut. Res.* 19 (2012) 2438–2447.
- [12] V.K. Gupta, A. Mittal, D. Jhare, J. Mittal, Batch and bulk removal of hazardous colouring agent rose bengal by adsorption techniques using bottom ash as adsorbent, *RSC Adv.* 2 (2012) 8381–8389.
- [13] A. Mittal, R. Jain, J. Mittal, M. Shrivastava, Adsorptive removal of hazardous dye quinoline yellow from wastewater using coconut-husk as potential adsorbent, *Fresen. Environ. Bull.* 19 (2010) 1–9.
- [14] H. Daraei, A. Mittal, M. Noorisepehr, F. Daraei, Kinetic and equilibrium studies of adsorptive removal of phenol onto eggshell, waste, *Environ. Sci. Pollut. Res. Int.* (2012), DOI: 10.1007/s11356-012-1409-8.
- [15] Muhammad, T.G. Chuah, Y. Robiah, A.R. Suraya, T.S.Y. Choong, Single and binary adsorptions isotherms of Cd(II) and Zn(II) on palm kernel shell based activated carbon, *Desalin. Water Treat.* 29 (2011) 140–148.
- [16] L. Zhirong, Y. Rong, S. Xinhui, Adsorption of Th (IV) by peat moss, *Desalin. Water Treat.* 28 (2011) 196–201.
- [17] D. Ozdes, A. Gundogdu, C. Duran, H.B. Senturk, Evaluation of adsorption characteristics of malachite green onto almond shell (*Prunus dulcis*), *Sep. Sci. Technol.* 45 (2010) 2076–2085.
- [18] X.S. Wang, F. Liu, H.J. Lu, P. Zhang, H.Y. Zhou, Adsorption kinetics of Cd (II) from aqueous solution by magnetite, *Desalin. Water Treat.* 36 (2011) 203–209.
- [19] A.P.A. Salvado, L.B. Campanholi, J.M. Fonseca, C.R.T. Tarley, J. Caetano, D.C. Dragunski, Lead(II) adsorption by peach palm waste, *Desalin. Water Treat.* 48 (2012) 335–343.
- [20] L. Zhang, H. Zhang, Y. Tian, Z. Chen, L. Han, Adsorption of methylene blue from aqueous solutions onto sintering process red mud, *Desalin. Water Treat.* 47 (2012) 31–41.
- [21] D. Ozdes, A. Gundogdu, B. Kemer, C. Duran, H.B. Senturk, M. Soyлак, Removal of Pb(II) ions from aqueous solution by a waste mud from copper mine industry: Equilibrium, kinetic and thermodynamic study, *J. Hazard. Mater.* 166 (2009) 1480–1487.
- [22] S.I.H. Taqvi, S.M. Hasany, M.I. Bhangar, Sorptive potential of beach sand to remove Ni(II) ions: An equilibrium isotherm study, *Clean—soil Air Water* 36 (2008) 366–372.
- [23] L. Zhang, S. Hong, J. He, F. Gan, Y.-S. Ho, Adsorption characteristic studies of phosphorus onto laterite, *Desalin. Water Treat.* 25 (2011) 98–105.
- [24] H.B. Senturk, D. Ozdes, A. Gundogdu, C. Duran, M. Soyлак, Removal of phenol from aqueous solutions by adsorption onto organomodified tirebolu bentonite: equilibrium, kinetic and thermodynamic study, *J. Hazard. Mater.* 172 (2009) 353–362.
- [25] J. Sheng, Y. Xie, Y. Zhou, Adsorption of methylene blue from aqueous solution on pyrophyllite, *Appl. Clay Sci.* 46 (2009) 422–424.
- [26] F. Bergaya, M. Vayer, CEC of clays: Measurement by adsorption of a copper ethylenediamine complex, *Appl. Clay Sci.* 12 (1997) 275–280.
- [27] APHA, Standard Methods for the Examination of Water and Wastewater, eighteenth ed., American Public Health Association, Washington, DC, 1985.
- [28] D. Ozdes, C. Duran, H.B. Senturk, Adsorptive removal of Cd (II) and Pb(II) ions from aqueous solutions by using Turkish illitic clay, *J. Environ. Manage.* 92 (2011) 3082–3090.

- [29] V.K. Garg, A. Moirangthem, R. Kumar, R. Gupta, Basic dye (methylene blue) removal from simulated waste water by adsorption using indian rosewood sawdust: timber industry waste, *Dyes Pigments* 63 (2004) 243–250.
- [30] K.G. Bhattacharyya, A. Sharma, Kinetics and thermodynamics of methylene blue adsorption on Neem (*Azadirachta indica*) leaf powder, *Dyes Pigments* 65 (2005) 51–59.
- [31] S. Lagergren, About the theory of so-called adsorption of soluble substance, *Kung Sven. Vetén. Hand.* 24 (1898) 1–39.
- [32] Y.S. Ho, G. McKay, Kinetic models for the sorption of dye from aqueous solution by wood, *J. Environ. Sci. Health., Part B: Process Saf. Environ. Prot.* 76 (1998) 183–191.
- [33] M. Al-Ghouti, M.A.M. Khraisheh, M.N.M. Ahmad, S. Allen, Thermodynamic behaviour and the effect of temperature on the removal of dyes from aqueous solution using modified diatomite: a kinetic study, *J. Colloid. Interf. Sci.* 287 (2005) 6–13.
- [34] W.J. Weber Jr., J.C. Morriss, Kinetics of adsorption on carbon from solution, *J. Sanitary Eng. Div. Am. Soc. Civ. Eng.* 89 (1963) 31–60.
- [35] S. Wang L. Li, H. Wu, Z.H. Zhu, Unburned carbon as a low-cost adsorbent for treatment of methylene blue-containing wastewater, *J. Colloid. Interf. Sci.* 292 (2005) 336–343.
- [36] B.H. Hameed, M.I. El-Khaiary, Kinetics and equilibrium studies of malachite green adsorption on rice straw-derived char, *J. Hazard. Mater.* 153 (2008) 701–708.
- [37] I. Langmuir, The adsorption of gases on plane surfaces of glass, mica and platinum, *J. Am. Chem. Soc.* 40 (1918) 1361–1403.
- [38] H.M.F. Freundlich, Über die adsorption in lösungen, *Z. Phys. Chem.* 57 (1906) 385–470.
- [39] M.J. Temkin, V. Pyzhev, Recent modifications to Langmuir isotherms, *Acta Physiochim. USSR* 12 (1940) 217–222.
- [40] M.M. Dubinin, L.V. Radushkevich, Equation of the characteristics curve of activated charcoal, *Chem. Zent.* 1 (1947) 875.
- [41] G. McKay, M. El-Guendi, M. Nassar, Equilibrium studies during the removal of dyestuffs from aqueous solutions using bagasse pith, *Water Res.* 21 (1987) 1513–1520.
- [42] F. Helfferich, *Ion Exchange*, McGraw-Hill, New York, NY, 1962.
- [43] Z. Al-Qodah, Adsorption of dyes using shale oil ash, *Water Res.* 34 (2000) 4295–4303.
- [44] J.M. Smith, H.C. Van Ness, *Introduction to Chemical Engineering Thermodynamics*, fourth ed., McGraw-Hill, Singapore, 1987.
- [45] R. Han, L. Zhang, C. Song, M. Zhang, H. Zhu, L. Zhang, Characterization of modified wheat straw, kinetic and equilibrium study about copper ion and methylene blue adsorption in batch mode, *Carbohydr. Polym.* 79 (2010) 1140–1149.
- [46] M.J. Jaycock, G.D. Parfitt, *Chemistry of Interfaces*, Ellis Horwood Limited, Chichester, 1981.
- [47] M. Horsfall Jr., A.A. Abia, A.I. Spiff, Kinetic studies on the adsorption of Cd^{2+} , Cu^{2+} and Zn^{2+} ions from aqueous solutions by cassava (*manihot sculenta cranz*) tuber bark waste, *Bioresour. Technol.* 97 (2006) 283–291.
- [48] G. Crini, H.N. Peindy, F. Gimbert, C. Robert, Removal of C.I. basic green 4 (malachite green) from aqueous solutions by adsorption using cyclodextrin-based adsorbent: Kinetic and equilibrium studies, *Sep. Purif. Technol.* 53 (2007) 97–110.
- [49] Y. Ozdemir, M. Dogan, M. Alkan, Adsorption of cationic dyes from aqueous solutions by sepiolite, *Microporous Mesoporous Mater.* 96 (2006) 419–427.
- [50] N. Tekin, O. Demirbas, M. Alkan, Adsorption of cationic polyacrylamide onto kaolinite, *Microporous Mesoporous Mater.* 85(3) (2005) 340–350.
- [51] F. Blockhaus, J.M. Sequaris, H.D. Narres, M.J. Schwuger, Adsorption-desorption behavior of acrylic-maleic acid copolymer at clay minerals, *J. Colloid. Interf. Sci.* 186 (1997) 234–247.